

# PRESENT STATUS OF THE HIGH TEMPERATURE ELECTROSTATIC LEVITATION TECHNOLOGY FOR CONTAINERLESS MATERIALS PROCESSING

Won-Kyu Rhim

Jet Propulsion Laboratory, California Institute of Technology, 4800 Oak Grove Drive, Pasadena, California 91109 USA

**ABSTRACT:** Present capabilities of the High Temperature Electrostatic Levitator (HTEL) for containerless materials processing are summarized. In studying high temperature materials, this technology utilizes electrostatic forces to isolate a sample material from the container walls in a high vacuum condition. Undercooled liquid states of various degrees are produced, and their thermophysical properties are measured using novel non-contact diagnostic methods. Amorphous as well as various crystalline phases may be accessed from deeply undercooled states and ensuing microstructure can be investigated. This technique can measure various thermophysical properties of metals, alloys, and semiconductors both in liquid and solid phases over a broad temperature range. At the present time the HTEL can measure the density, the thermal expansion coefficient, the ratio of the specific heat to the hemispherical total emissivity, the surface tension, and the viscosity.

## 1. INTRODUCTION

In the High Temperature Electrostatic Levitator (HTEL) a sample is levitated in a high vacuum by controlling applied electrostatic forces. Levitated sample is melted, and various experiments are performed over a broad temperature range around its melting temperature. Since the sample is well isolated in a high vacuum, the sample purity is preserved, and the molten drop can reach highly undercooled states. Once molten state is prepared, appropriate non-contact diagnostic techniques can be applied to measure various thermophysical properties at different temperature. Furthermore, it makes possible to investigate nucleation mechanism as well as formation of metastable crystalline and amorphous phases.

Some of useful characteristics of the HTEL are: (i) it can process various materials which include metals, semiconductors, and insulators, (ii) the sample heating and levitation mechanisms are completely decoupled, therefore, the range of sample temperature is not limited by the levitation mechanism, (iii) the processing environment being a high vacuum, sample cooling in the absence of heating can be rigorously described by a purely radiative heat transfer equation, (iv) the employment of feedback control allows quiescent sample positioning, and (v) it provides an open environment so that a sample can be viewed by various non-contact diagnostic instruments.

In this paper, the present status of the HTEL as applied in the areas of thermophysical properties, nucleation mechanisms, and metastable phases is described. Since the first paper on the HTEL was published in 1993 [1], its capabilities for thermophysical property measurements of molten materials have been substantially extended to include measurement of the density, thermal expansion coefficient, surface tension, viscosity, specific heat and hemispherical total emissivity. These capabilities have been applied in numerous materials, and it is the intent of this paper to give a brief summary of these progress.

## II. THE HTEL FOR CONTAINERLESS MATERIALS PROCESSING

### J. Mass Density and Thermal Expansion Coefficient

The HTEL provides a desirable condition for the density measurement from a levitated drop. First of all, the HTEL shows stable levitation and allows the drop to reach a deeply undercooled state. Secondly, the shape of a levitated drop in a HTEL is axi-symmetric around the vertical direction. Therefore, a single side image of the drop contains full information about the drop volume. The density measurements system which was recently developed at JPL seems to support this. The underlying definitions for the density  $\rho$  and the thermal expansion coefficient  $\beta$  are

$$\rho = \frac{m}{V}, \quad \text{and} \quad \beta = \frac{1}{V} \frac{dV}{dt},$$

where  $m$  is the sample mass,  $V$  is the sample volume, and  $T$  is the sample temperature,

The system consisted of a high quality tele-microscope to get a magnified side view of a levitated drop, ii CCD video camera attached to the microscope, a video recording system, and a mini-computer for image digitization and analysis. Image analysis software was developed to extract the image area accurately. The basic density measurement technique using the IITFSL is described in detail by Chung et al in the reference [2]. Fig. 1 shows a density data for a molten nickel, and it was compared with other results measured by conventional methods. [3, 4] The starting point of the experiment was the nickel sample overheated about 100K above the melting point. Upon blockage of the heating source, the melt was allowed to cool radiatively while the sample images were recorded at the rate of 30 frames per second. The melt undercooled more than 300K before recalescence took place. At the present time this technique can measure density with less than 0.2 % error. In other materials, Rhim et al and Ohsaka et al measured the densities of a solid and a molten silicon [5,6]. Recently, for the first time, the density of an easily glass forming alloy  $\text{Zr}_{41.2}\text{Ti}_{13.8}\text{Cu}_{12.5}\text{Ni}_{10.0}\text{Be}_{22.5}$  was measured by Ohsaka et al. [7]

## 2. Surface Tension and Viscosity

Surface tension and viscosity play important roles in fluid processing of engineering significance. Surface tension influences both thermodynamic and hydrodynamic behavior of fluid surface during casting, welding, melt spinning, and laser melting. In the presence of temperature or concentration gradient, the resultant surface tension gradient gives rise to Marangoni flow which can have significant effects, for instance, in the floating zone crystal growth in the reduced gravity environment,

Surface tension is a surface property, defining the excess free energy required to create a unit area of free surface for a given amount of fluid mass. This energy is needed, because atoms or molecules on the surface are at higher energetic states than those in the bulk. Usually, surface tension is measured by either the sessile-drop [8] or pendant-drop [9] methods, which are not applicable to highly reactive melts. Non-contact methods not only avoid direct contact with crucibles, thus preventing surface contamination, it also allows the melt to reach deeply undercooled state whose properties affect the phase transformation process and the resulting microstructure.

Viscosity on the other hand is related to the atomic or molecular diffusion. Viscosity influences many important processes such as undercooling and nucleation, solidification of eutectic alloys, Ostwald ripening, anti separation of immiscible liquids. In particular, understanding the role played by viscosity during glass formation processes will be very important for the development of various glass forming alloys bearing valuable physical and chemical properties.

Spherical shape of a molten sample levitated by the IITFSL provides an ideal condition to measure the surface tension and the viscosity with great accuracy. In view of the fact that surface tension is particularly sensitive to even minute surface contamination, a IITFSL operating in a high vacuum environment would be ideal for the surface tension measurements. If a liquid has small viscosity in a weak damping limit, the free oscillation of a drop can be expressed by

$$r(t) = r_0 + \sum_n r_n \cos(\omega_n t) P_n(\cos \theta) \exp\left(-\frac{t}{\tau_n}\right), \quad (1)$$

where  $r_0$  is the radius of the drop when it is spherical,  $r_n$ , and  $\omega_n$  are respectively the oscillation amplitude and the angular frequency of the  $n$ -th mode,  $P_n(\cos \theta)$  is the Legendre polynomial of

order  $n$ ,  $\theta$  is the angle measured between  $z$  axis and the radial direction, and  $\tau_n$  is the damping time constant of the  $n$ -th mode. Assuming uniform charge distribution over the drop surface and the drop is oscillating at  $n=2$  mode, the surface tension is determined by the formula derived by Rayleigh [10]

$$\sigma = \frac{r_o^3 \rho}{8} (\omega_2^2 + \frac{Q_s^2}{8\pi^2 r_o^6 \rho \epsilon_o}). \quad (2)$$

in the HTESI, the voltage difference between the top and the bottom electrodes is inversely proportional to the sample charge. Since the sample mass  $m$ , the sample position, the distance between electrodes  $d$ , and the applied voltage  $s$   $V$  are known, the approximate sample charge value can be obtained from the force balance equation  $Q_s V/d = mg$ . For more accurate values one should go through numerical analysis taking into account various non ideal conditions such as the size and shape of the electrodes and the size and the position of the sample. From the damping time constant  $\tau_2$  for  $n=2$ , the viscosity  $\eta$  is obtained by [11]

$$\eta = \frac{\rho r_o^2}{5\tau_2}. \quad (3)$$

Technology verification for the surface tension measurement has been successfully carried out in molten tin, lead, and silicon [5]. Both surface tension and viscosity have been measured in an eutectic Ni-Zr alloy [12] and several boron doped silicon [13]. Fig. 2 shows a transient oscillation of a molten Zr-Ni alloy freely oscillating at  $n=2$  mode. The oscillation frequency is related to the surface tension through Eq. (2) while the damping time constant (or the spectral line width) is related to the viscosity through Eq. (3). The basic concept of this technique was published in the reference [14], and a more detailed description which includes effects of non-idealities caused by uneven surface charge density [15] is being prepared for a future publication [16].

### 3. Specific Heat Capacity and Total Hemispherical Emissivity

The specific heat capacity plays an important role for the evaluation of steady state nucleation rate as well as undercooling limit in a liquid state. It not only appears explicitly in the classical nucleation rate equation, it also appears implicitly through the Gibbs free energy difference  $\Delta G_v$  since the free energy is determined if the heat capacity is known. Experimental data of the heat capacity of undercooled liquid, although they are extremely valuable, have been lacking.

The total hemispherical emissivity of a sample material,  $\epsilon_T$ , is defined by the ratio between the hemispherical total emissive power [11] to that of a black body, i.e.

$$\epsilon_T = \frac{H}{\sigma_{SB} T^4}. \quad (4)$$

For example,  $\epsilon_T$  is needed to determine the thermal environment during crystal growth in the floating zone growth system, and also in determining the cooling rate of atomized droplets in the rapid solidification processing. In spite of their importance,  $c_p$  and  $\epsilon_T$  are known for very few high-temperature liquids. Data is particularly scarce for undercooled liquids since they cannot be reached using conventional methods. In a HTESI, a levitated molten sample cools radiatively in

the vacuum environment. From the radiative heat transfer equation, the expression for  $c_p/\epsilon_T$  can be obtained as:

$$\frac{c_p}{\epsilon_T} = -\frac{6\sigma_{SB}(T^4 - T_s^4)}{\rho d \frac{dT}{dt}} \quad (5)$$

where  $p$  is the sample mass density, ' $T$ ' is the sample temperature,  $T_s$  is the temperature of surroundings,  $\sigma_{SB}$  is the Stefan-Boltzmann constant, and  $d$  is the sample diameter. The fact that accurate measurement of  $\epsilon_T/c_p$  is possible from Eq. (5) upon measurement of  $dT/dt$  is one of the most important merits of containerless processing by the LMFSL. Any additional heat inputs (such as residual rf heating in the case of electromagnetic levitation) and heat loss (such as conductive and convective heat loss if a gaseous cooling agent is used), which are usually not well defined, will lower the accuracy of the  $\epsilon_T/c_p$  measurements.

From  $c_p(T)/\epsilon_T(T)$  data,  $c_p(T)$  can be determined if  $\epsilon_T(T)$  is known. Likewise,  $\epsilon_T(T)$  can be determined if  $c_p(T)$  is known. Strictly speaking  $\epsilon_T(T)$  has to be measured independently over the entire temperature range. However,  $C_p(T_m)$  at melting temperature is often available, or  $c_p(T_m)$  is easier to measure using a conventional calorimeter than to measure  $\epsilon_T(T_m)$  under the present techniques capabilities. In that case,  $\epsilon_T(T_m)$  is determined using available  $c_p(T_m)$ . Since  $\epsilon_T(T)$  is known to be weakly temperature dependent, an assumption  $\epsilon_T(T) \approx \epsilon_T(T_m)$  can be made over a few hundred K around  $T_m$ , and the  $c_p(T)$  is determined in that temperature range. This approach has been applied to nickel and zirconium [17], to silicon [18], and to the glass forming alloy  $Zr_{41.2}Ti_{13.8}Cu_{12.5}Ni_{10.0}Be_{22.5}$  [19].

#### 4. Studies of Nucleation from Undercooled Liquids

Since samples are processed in a clean environment of vacuum, sample purity is preserved, and further purification might even be taking place as volatile impurities leave the sample as the sample is kept at a high temperature. Furthermore, in the absence of appreciable internal flow unlike the case of the electromagnetic levitation, one can safely rule out the dynamic nucleation. Spontaneous nucleation phenomena are basically statistical in nature. Experimentally a liquid drop above its melting temperature is allowed to cool radiatively toward the room temperature and to record the temperature at the nucleation event. This process has to be repeated over 100 times to accumulate enough data for statistical analysis. Our undercooling/nucleation studies using two different grades of zirconium consistently revealed single nucleation mechanism in contrast to the results obtained by electromagnetic levitators and drop tubes [20, 21].

With the heating source turned off, the maximum cooling rate of a sample depends on its size and optical property. Study of undercooling and nucleation as a function of cooling rate may be possible with a slight modification of the current system to accommodate various size samples. Deep undercooling and rapid solidification make it possible to form metastable phases with novel microstructures which are not allowed by conventional solidification processing. In simplistic terms, metastable phase nucleation is determined by the liquid undercooling level while morphological development is controlled by solidification velocity. Combination of a high speed imaging system and a pyrometer will allow measurement of solidification velocities as a function of temperature which is invaluable for the study of solidification and the understanding of novel microstructure formation.

## 5. Metastable Phases

A glass is formed from a liquid if nucleation of a solid is avoided during cooling process. The degree of glass formability is often expressed by the critical cooling rate for glass formation. The critical cooling rate widely varies from 108 K/sec to 1K/sec depending on the elements and their compositions. In order to determine the critical cooling rate, the first step is to construct the continuous cooling transformation (CCT) curve for solid nucleation. CCT curve is constructed by measuring the nucleation temperatures as a function of the constant cooling rate. The critical cooling rate for glass formation is the slowest rate at which the solid is not nucleated. As an initial demonstration we have used a glass forming alloy  $Zr_{41.2}Ti_{13.8}Cu_{12.5}Ni_{10.0}Be_{22.5}$  and measured the minimum cooling rate [22], specific heat, and hemispherical total emissivity [19]. More recently the whole Time-Temperature-Transformation ('TTT') curve was successfully measured for this material [23]. With a built-in cooling-rate-control capability, the HTFSL will become invaluable for the development of easily glass forming alloys.

## ACKNOWLEDGMENTS

The author would like to thank S. K. Chung, D. Barber, G. Gutt, R. E. Spjut, K. F. Man, A. J. Rulison, Y. J. Kim, and K. Ohsaka for their contributions for the development and applications of the HTFSL technologies. This work was carried out at the Jet Propulsion Laboratory, California Institute of Technology, under contract with the National Aeronautics and Space Administration. Reference herein to any specific commercial product, process, or service by trade name, trademark, manufacturer, does not constitute or imply its endorsement by the United States Government or the Jet Propulsion Laboratory, California Institute of Technology.

## REFERENCES

- [1] Rhim WK, Chung SK, Barber D, Man KF, Gutt, Rulison AJ, Spjut RE. An Electrostatic levitator for high temperature containerless materials processing in 1-g. Rev. Sci. Instrum. 1993, 64, 2961-2970
- [2] Chung SK, Thiessen D, and Rhim WK. A non contact measurement technique for the density and thermal expansion of molten materials. Rev. Sci. Instrum. September 1996 (in press)
- [3] Kirchenbaum AD, Cahill JA. Trans. ASM 1963, S6, 281
- [4] Lucas LD. Doctoral thesis, 1962, Univ. Paris
- [5] Rhim WK, Chung SK, Rulison AJ, Spjut RE. Measurements of thermophysical properties of molten silicon. Int. J. Thermophysics, 1996 (in press)
- [6] Ohsaka K, Chung SK, Rhim WK, Holzer JC. Densities of Silicon Determined by an image Digitizing Technique in Combination with an Electrostatic Levitator. Appl. Phys. Letters, 1996 (submitted)
- [7] Ohsaka K, Chung SK, Rhim WK, Peker A, Scruggs D, Johnson WL. Specific volume of the  $Zr_{41.2}Ti_{13.8}Cu_{12.5}Ni_{10.0}Be_{22.5}$  alloy in the liquid, glass and crystalline states. Appl. Phys. Letters, 1996 (submitted)
- [8] Sangiorgi R, Carracciolo G, Passerone A. J. Mater. Sci. 1982, 17, 2895
- [9] Thiessen DB, Man KF. Proc. 12th Symp. on Thermophysical Properties, June 19-24, 1994
- [10] Lord Rayleigh, Phil. Mag. 1882, 14, 184
- [11] Lamb H. Hydrodynamics, 6th ed., Cambridge University Press, 1932
- [12] Rhim WK, Rulison AJ, Lee D, Johnson WL. Thermophysical Properties of a Zr-Ni Eutectic Alloy (in preparation)
- [13] Ohsaka K, Rhim WK, Holzer JC. Surface tension and viscosity of molten silicon doped with boron (in preparation)
- [14] Rhim WK, Rulison AJ. Surface tension and viscosity measurements of molten materials by electrostatic levitation. NASA Tech Brief July 1996, 64-65

- [15] Feng JQ, Beard KV. Small-amplitude oscillations of electrostatically levitated drops. *Proc. R. Soc. Lond. A*, 1990, 430, **133-150**
- [16] Rhim WK, Spjut RL. Surface tension and viscosity measurement by electrostatic levitation (in preparation)
- [17] Rulison AJ, Rhim WK. A non-contact measurement technique for the specific heat and total hemispherical emissivity of undercooled refractory materials. *Rev. Sci. Instrum.* 1994, 65, 695-700
- [18] Rulison AJ, Rhim WK. Constant pressure specific heat to hemispherical total emissivity ratio for undercooled liquid nickel, zirconium, and silicon. *Metal. and Materials Trans. B*, 1995, 26, 503-508
- [19] Busch R, Kim YJ, Johnson WL, Rulison AJ, Rhim WK, Isheim D. Hemispherical total emissivity and specific heat capacity of deeply undercooled  $Zr_{41.2}Ti_{13.8}Cu_{12.5}Ni_{10.0}Be_{22.5}$  melts. 1995, 66, 3111-3113
- [20] Morton CW, Hofmeister WI, Bayuzick RJ, Robinson MB. *Materials Science and Engineering A*, 1994, 178, 209-215
- [21] Rulison AJ, Rhim WK, Bayuzick RJ, Hofmeister WI, Morton CW. Containerless liquid to solid nucleation pathways in two representative grades of commercially available zirconium, *Acts Metallurgic et Materialia* (in press)
- [22] Kim YJ, Busch R, Johnson WL, Rulison AJ, Rhim WK. Metallic glass formation in highly undercooled  $Zr_{41.2}Ti_{13.8}Cu_{12.5}Ni_{10.0}Be_{22.5}$  during containerless electrostatic levitation processing, *Appl. Phys. Letts.* 1994, 65, 2136
- [23] Kim YJ, Busch R, Johnson WL, Rulison AJ, Rhim WK. Experimental determination of a time-temperature-transformation diagram of the undercooled  $Zr_{41.2}Ti_{13.8}Cu_{12.5}Ni_{10.0}Be_{22.5}$  alloy using the containerless electrostatic levitation processing technique. *Appl. Phys. Lett.* 1996, 68, 1057-1059

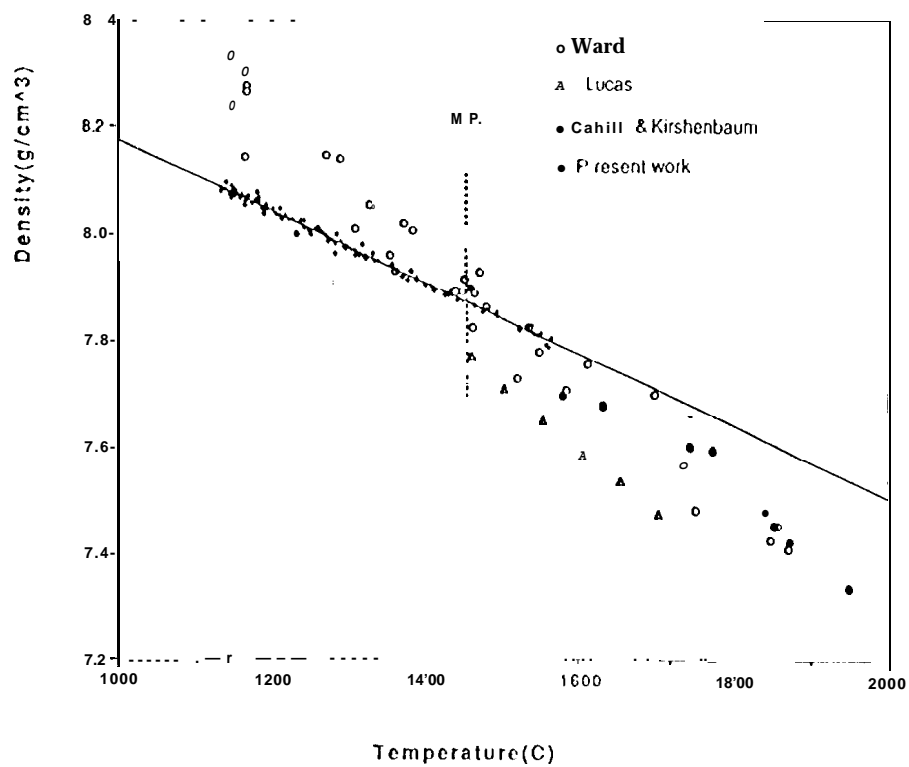


**Fig. 1** Density data for pure nickel as the melt was continuously cooled while levitated by HTESL(+), and these are compared with other results measured by conventional methods.

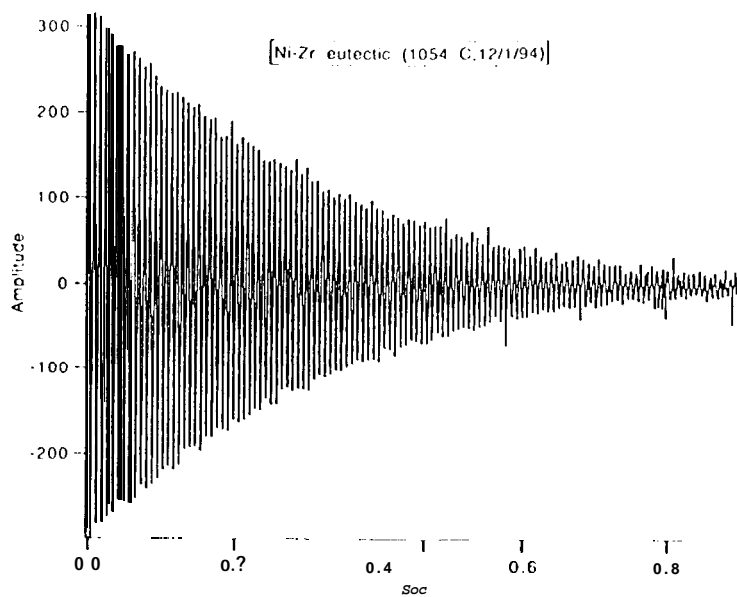


**Fig. 2** A molten Zr-Ni alloy freely oscillating at  $n=2$  mode.